Engineering Journal issn: 0125-8281

Article

Effective Solar Light Photocatalysis by Graphene Sheets (GSs) Addition on the Composite TiO_2/SiO_2

Mia L. Ayuningtyas[1,a], **Sukasem Watcharamaisakul**[1,b], **and Supunnee Junpirom**[2,c,*]

1 School of Materials Engineering, Institute of Engineering, Suranaree University of Technology, Nakhon Ratchasima 30000, Thailand
2 School of Chemical Engineering, Institute of Engineering, Suranaree University of Technology, Nakhon Ratchasima 30000, Thailand
E-mail: [a]d58400083@g.sut.ac.th, [b]sukasem@sut.ac.th, [c,*]supunnee@sut.ac.th (Corresponding author)

Abstract. This study investigated the synthesis of TiO_2/SiO_2 by using a sol-gel method with the addition of difference of the mass ratio of Titanium (Ti):Graphene Sheets (GSs) (1:0; 1:0.04; 1:0.07; 1:0.14) and the variation of calcination temperature (Tcal) (400 ℃; 450 ℃; 500 ℃). The synthesized composites were analyzed by X-ray powder diffraction (XRD) and Scanning electron microscope and energy dispersive X-ray spectrometer (SEM-EDS). The TiO_2/SiO_2/GSs XRD pattern shows anatase and rutile phases as well as graphite at the near point of 2θ (26°-27°). The tendency of anatase phase according to GSs ratio and Tcal variables is decreasing with an increase in the GSs ratio and Tcal. The crystal size was in the range of 24 – 41 nm. The decolorization of methylene blue was done under four conditions: dark, UV lamp, LED, and solar light. The photocatalytic activity result under solar light is comparable with UV light. The photocatalyst with a ratio at 0.07 and Tcal at 450 ℃ gave the maximum efficiency of MB decolorization under solar light with 97.83 % within 3 hours. The reusable TiO_2/SiO_2/GSs show a slight fall in efficiency after four cycle times.

Keywords: Photocatalyst, graphene sheet, TiO_2/SiO_2, sol-gel method.

ENGINEERING JOURNAL Volume 25 Issue 6
Received 23 November 2020
Accepted 5 June 2021
Published 30 June 2021
Online at https://engj.org/
DOI:10.4186/ej.2021.25.6.1

DOI:10.4186/ej.2021.25.6.1

1. Introduction

The photocatalyst is the material that can accelerate photoreaction without being consumed as a reactant [1–3]. While it can also be defined more as a material that absorbs light quanta and provides chemical transformation repeatedly, coming into intermediate reaction and regenerating its composition [4–6]. Photocatalyst has two main stages: (i) adsorption of the reactants on to catalyst surface and (ii) photocatalytic activity of catalyst as a reaction with reactants. The reactant adsorption on the surface of the photocatalyst has a crucial role in the photocatalytic activity mechanism [7–10].

Titanium dioxide (TiO_2) is the semiconductor material that is widely used as photocatalyst for the degradation of several pollutants. Semiconductor materials have a bandgap between conducting band and valence band [11]. These bands determined the electrical conductivity of materials. When the light in a certain wavelength illuminated TiO_2, that energy will induce the electrons on valence band to excited into conducting band. These free electrons will move along the surface or near the surface of TiO_2 yet the hole of electrons is in the valence band [12,13].

TiO_2 is the most widely used photocatalyst among them. TiO_2 has attracted attention because of its desirable physicochemical properties such as thermal and chemical stability, relatively high photocatalytic activity, low toxicity, and low cost. However, the bandgap of TiO_2 is generally a range of 3.0-3.2 eV [1, 14], which gives work range as photocatalyst under UV range (100 – 400 nm). It almost makes TiO_2 cannot effectively work under the radiation of solar light (only 3-5 % of the solar spectrum) [15].

Somehow, nonmetal doping was effective to obtain a visible light response. In recent years, carbon in graphene form is popular doping material to decrease the bandgap of semiconductors, especially in photocatalyst applications. The graphene is considered as an impurity in TiO_2 structural system, the bandgap of graphene will overlap with TiO_2, in this case, the conduction band of graphene will be lower than TiO_2 then it will decrease the gap between the conduction band of graphene and valence band of TiO_2 [16]. Its properties such as the large BET area (which providing more active adsorption sites), chemical inertness, zero bandgap (which acting as a sensitizer), high electron mobility (which prolong electron lifetime), electron storage ability (playing as an electron tank), and tunable structural give another advantage to modified the photocatalysts [17, 18]. Therefore, the composite of graphene and semiconductors, especially TiO_2, is currently being considered as a potential photocatalyst in air and water purification. The graphene based TiO_2 composite exhibit enhanced photocatalytic activity in comparison with only TiO_2 [19].

Photocatalyst in the case of environmental purification will act as adsorbent and photocatalyst. Those actions take place at the same time. Since the photocatalytic reaction will take place mostly near the surface of photocatalyst. To enhance the adsorptive of TiO_2, SiO_2 will be added to increase the surface area for adsorption [20]. SiO_2 also is known as the material that can improve the photocatalytic process of TiO_2 [21].

The aim of this work is mainly focused on the effect of the addition of GSs on TiO_2/SiO_2 photocatalyst in terms of the change of structure and work range of photocatalytic processes. The preparation of TiO_2/SiO_2 has been studied under Klondon work [22]. The variables were the amount of GSs and the calcination temperature (Tcal). The effects of these variables on the methylene blue degradation during photocatalysis with a variation of applied light sources e.g. dark, UV lamp, LED lamp, and solar light were investigated.

2. Materials and Methods

2.1. Preparation of $TiO_2/SiO_2/GSs$

10 mL of Ti-n-butoxide is diluted by 35 mL of absolute ethanol, became solution A. Then the mixture of 3 mL of HNO_3 concentrated, 35 mL of absolute ethanol and 10 mL of deionized water, called solution B. GSs pure was added into solution B with mass ratio Ti:GSs (1:0; 1:0.04; 1:0.07; 1:0.14) are labeled as G0; G0.04; G0.07; and G0.14 respectively. The SiO_2 was added into the mixed solution to make the ratio of TiO_2:SiO_2 is 1:1. SiO_2 that be used was prepared from rice husk with H_2SO_4, as published in Klondon work [22].

$TiO_2/SiO_2/GSs$ photocatalyst was synthesized by the sol-gel method. Solution B with the variation ratio of GSs was added into solution A slowly under stirring and stirred for 1 hour. 1.5 g of SiO_2 was added under stirring then kept the solution for one day. Finally, the solution is drying at 110 ℃ for 12 hours. This sample continues to calcine with the variation of temperature from 400 ℃, 450 ℃, and 500 ℃ (sample coding T400, T450, and T500 respectively) for 6 hours. The composite photocatalyst of $TiO_2/SiO_2/GSs$ was finally obtained.

2.2. Characterization of $TiO_2/SiO_2/GSs$

The identification of the crystal phase of the composite was performed using a Bruker D2 PHASER XRD. In titanium dioxide, XRD provides information about the major peaks of the structure phase of TiO_2. The major peaks of pure anatase at 2θ consist (101), (004), (200), (105), (204), (220), and (215) planes. Meanwhile for rutile have intensity at (110), (101), (200), (111), (210), (211) and (220) planes [18, 23, 24]. The XRD patterns show different peak broadening which inversely proportional to the average crystal size of $TiO_2/SiO_2/GSs$ according to Scherrer equation [15, 16] as in Eq. (1)

$$D_p = \frac{K\lambda}{\beta\cos\theta} \quad (1)$$

where Dp is the crystal size (nm), K is the Scherrer constant, like 0.89 for cubic crystallite shape [25], λ is the x-ray wavelength (Cu Kα radiation source, 0.154178 nm), β is the full width at half maximum (FWHM), and θ is the

diffraction angle (2θ of peak (101) of anatase is 25.30°). The ratio between crystal phase of TiO_2 also can be calculated from XRD result by following equation [15, 26]

$$\% \text{ of anatase phase} = \frac{100}{1+(I_R/0.791I_A)} \quad (2)$$

where IR and IA are the strongest intensities of rutile and anatase phase, respectively.

The structure of TiO_2/SiO_2/GSs was characterized by using FE-SEM JEOL JSM 7800F to analyze surface properties. The detector that was used is a backscattering detector because the sample has a high atomic number which backscattered electrons stronger thus appear brighter in the image. It can detect the contrast between areas with different compositions. EDS was used in conjunction with SEM to characterize the elemental composition. After an electron beam bombarded the sample, a relative abundance of x-ray emitted from the sample be measured by the detector to determine the element composition of sampled volume. The samples were labeled by their ratio G0, G0.04, G0.07, and G0.14 with T400, T450, T500 as represented to Tcal 400 ℃, 450 ℃, and 500 ℃, respectively.

2.3. Photocatalytic Activity

The photocatalytic activity of the TiO_2/SiO_2/GSs was investigated by using the degradation of Methylene Blue (MB) solution. The MB solution was prepared by dissolved 20mg of methylene blue ($C_{16}H_{18}N_3SCl$) with 1L of deionized water to be stock solution 20 mg/L. This solution then was diluted to be standard from 2, 4, 6, 8, and 10 mg/L, also the initial condition (2.5 mg/L) for photocatalytic reaction.

The initial condition was done by analyzing the degradation of MB by variation of the amount of photocatalyst (0.05 g; 0.1 g; and 0.15 g) in a 100 mL MB solution of 2.5 mg/L under solar light. The initial concentration of MB also was determined by put 0.1 g of the photocatalyst into 100 mL MB solution of 1 mg/L, 2.5 mg/L, and 4 mg/L.

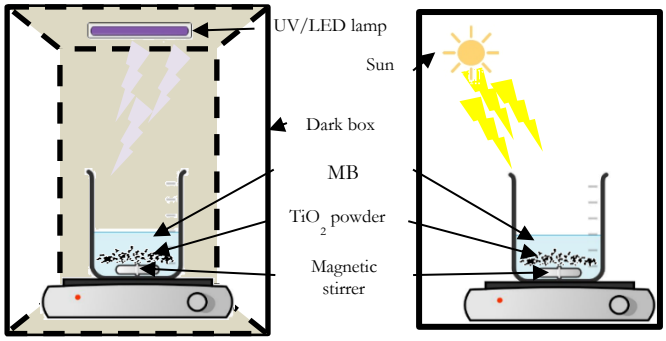

Fig. 1. Experimental setup for Methylene Blue decolorization by TiO_2 photocatalyst in the dark box (left) and with different light sources (left) and an open system under solar light (right).

The 0.1 g of the composite was put into a 100 mL solution of 2.5 mg/L of MB in the reactor under the different applied light sources, e.g., UV lamp, LED lamp, and solar light. The dark condition was also tested to show how the adsorption takes place in photocatalyst when it has no light source. The UV lamp that is used has power 4 W and wavelength 366 nm while an LED lamp has power 35 W and wavelength 557 nm. The monitoring under solar light was restricted from 11 am to 4 pm according to peak sun-hours in Thailand (5 hours). The interval of measurement of MB concentration change was in every 30 minutes for 3 hours of data.

The 5 mL of decolorization solution was analyzed by using a T80+ PG instrument UV-Vis spectrophotometer with absorbance at a wavelength of 665 nm. The photocatalytic activity was measured as the decolorization of MB by the following equation:

$$\%\text{decolorization} = \frac{C_0-C_t}{C_0} \times 100\% \quad (3)$$

where C_0 and C_t are the initial concentration and concentration at the time of MB, respectively. The variation of catalyst loading (0.05 to 0.15 g of TiO_2/SiO_2/GSs) and the initial concentration of MB (1 to 4 mg/L) were investigated. The photocatalytic activity of optimum condition was also measured with three-time cycles.

The kinetics of photocatalytic degradation of MB was based on the most used Langmuir-Hinshelwood (LH) kinetics, is given by:

$$r = -\frac{dC}{dt} = \frac{k_r KC}{1+KC} \quad (4)$$

where r is the rate reaction (mg/L min) that changes by time t (min), C is the concentration at any time during degradation (mg/L), k_r is limiting rate constants of reaction at maximum coverage, and K is the equilibrium constant for adsorption of the substrate onto catalyst [27].

The integrated expression of this equation can calculate the constant k_r and K in Eq. (4) by limit $C = C_0$ at $t = 0$ and $C = C$ at $t = t$. the integrated can be expressed:

$$\ln\left(\frac{C_0}{C}\right) + K(C_0-C) = k_r Kt \quad (5)$$

The LH kinetics on the first order has condition $KC<<1$. If so, Eq. (4) becomes $r=k_rKC$ and be integrated into first-order kinetics and is given by:

$$\ln\frac{C_0}{C_t} = kt \quad (6)$$

where k (k_rK)is the rate constant (min^{-1}) and t is the degradation time (min).

Since in photocatalyst, there are two process simultaneously occur (adsorption-desorption and degradation), kinetic models need to consider the

transformation of MB to adsorbed MB (MB_{TiO2}) and to photodegraded product (MB_{pr}) processes as well [28]. The processes can be described as in the work of Giovannetti et al. [28], as following;

$$MB+TiO_{2\ comp} \rightarrow MB_{TiO_2} \quad (7)$$

$$MB_{TiO_2}+hv \rightarrow MB_{pr} \quad (8)$$

The kinetics of MB decreased and the formation of MB_{TiO2} and MB_{pr} is given by:

$$-\frac{d[MB]}{dt}=k_1[MB] \quad (9)$$

$$\frac{d[MB_{TiO_2}]}{dt}=k_1[MB]-k_2[MB_{TiO_2}] \quad (10)$$

$$\frac{d[MB_{pr}]}{dt}=k_2[MB_{TiO_2}] \quad (11)$$

b By integrated Eq. (9) into $[MB]_t=[MB]_0e^{-k_1t}$ and substituted into Eq. (10), can be obtained:

$$\frac{d[MB_{TiO_2}]}{dt}=k_1[MB]_0e^{-k_1t}-k_2[MB_{TiO_2}] \quad (12)$$

and integrated to become:

$$[MB_{TiO_2}]=\frac{k_1}{k_2-k_1}(e^{-k_1t}-e^{-k_2t})[MB]_0 \quad (13)$$

During the process at any time *t*, $[MB_{pr}]=[MB]_0-[MB]_t-[MB_{TiO_2}]_t$, then substitute with integration Eq. (9) and Eq. (12) may be obtained:

$$[MB_{pr}]=\left\{1+\frac{k_1e^{-k_2t}-k_2e^{-k_1t}}{k_2-k_1}\right\}[MB]_0 \quad (14)$$

3. Result and Discussion

3.1. The Characterization of $TiO_2/SiO_2/GSs$

The phase of TiO_2 was known to affects the ability of TiO_2 as photocatalyst. XRD characterized the crystal phase of the composite of $TiO_2/SiO_2/GSs$ while FE-SEM/EDS analyzed the physical structure and elemental components. The EDS result was showed on the %w of Ti and C presence, which was analyzed on 5 points for each sample and presented as mean data. The preparation, especially for the ratio composition and calcination treatment, gives the effect into its surface properties.

3.1.1. Effect of GSs ratio

XRD result in Fig. 2(a) can be used to know how the proportion of TiO_2 and GSs for each sample, based on their strongest intensity. The XRD patterns of the sample based on the amount of GSs also show a tendency of intensity and a decrease in FWHM, which means that an increase in crystal size. The crystal size of the $TiO_2/SiO_2/GSs$ composite was in the range of 25-40 nm, as to be presented in Fig. 2(b). The GSs induce the TiO_2 phase change from anatase to rutile in the form of their bonding between TiO_2 and GSs.

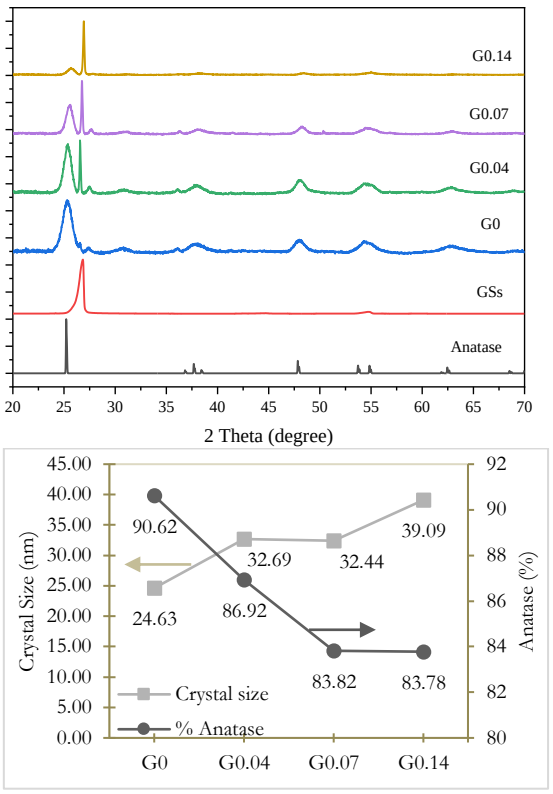

Fig. 2. (a) XRD pattern of TiO_2 photocatalyst with a variation of GSs ratio (T450 ℃) and (b) the interpretation data of the XRD result.

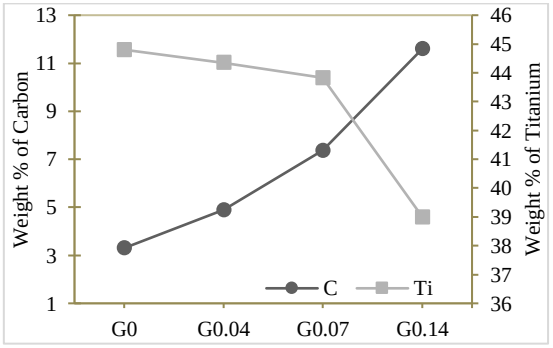

Fig. 3. EDS result of $TiO_2/SiO_2/GSs$ at Tcal 450 ℃.

From the EDS results, it is shown that the increasing amount of C concerning the increasing of GSs ratio as it is seen in Fig. 3. The carbon content in the spectrum of sample G0 may be the result of the residue of raw materials used to prepare the sample. On the other hand, Ti (titanium) presence decrease, adjust with the presence of C content. From these investigations can be concluded that the increase in the GSs results in the larger crystal size and the continuous phase change from anatase to rutile.

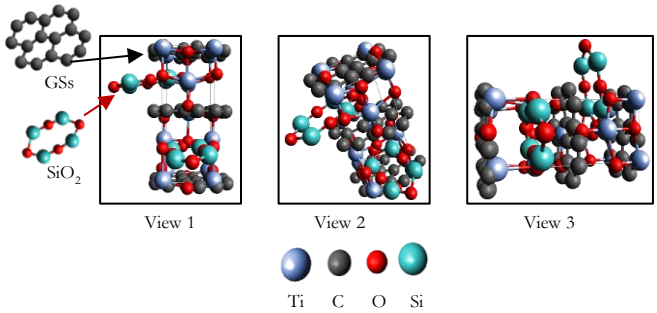

Fig. 4. The proposed structural model of $TiO_2/SiO_2/GSs$ in a one-unit cell of anatase phase.

The result of both XRD and EDS can be speculated as to the structural model, as displayed in Fig. 4. The C that is modeled based on GSs is possible to be bonded to the oxygen on TiO_2 as the reaction heat was lower than the minimum carbide to be formed (1200 ℃) [29]. The more C on GSs, the more unit cell is stretched and make crystal lattice bigger than the original one and enhance the phase change from anatase to be the more stable rutile phase. The presence of SiO_2 also is bonded to TiO_2, resulting in bonding between oxygen-oxygen. The SEM images support the layering of GSs on TiO_2 composite as in Fig. 5.

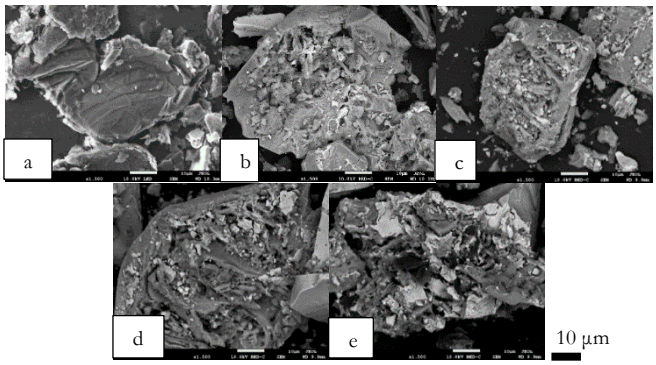

Fig. 5. SEM images of (a) GSs and $TiO_2/SiO_2/GSs$ composite (b) G0, (c) G0.04, (d) G0.07 and (e) G0.14 at Tcal 450 ℃.

The SEM images of the composite $TiO_2/SiO_2/GSs$ were characterized, and it is exhibited in Fig. 5. As depicted in Fig. 5(a), the graphite sheets (GSs) are observed as the ordered layers structure with an irregular shape. This property affects the $TiO_2/SiO_2/GSs$ pattern, which tends to have layers because of the GSs presence. The composite pattern is shown in Figure 5(b-e) for the ratio of G0, G0.04, G0.07, and G0.14, respectively.

3.1.2. Effect of calcination temperature (Tcal)

Calcination has another role in affecting the performance of the material. In TiO_2 preparation, Tcal affects the structure phase of anatase and rutile, especially based on their phase transition. The result in Fig. 6(a) shows that a pure anatase phase exists at a lower temperature until T450 when rutile peak is observed and increases along with the increase in Tcal. It explains how the tendency of TiO_2 that stays as anatase phase at a lower temperature in the phase diagram and starts to transform into rutile at a higher temperature, as presented in Fig. 6(b). This temperature gives energy into TiO_2 bonding to change form from metastable one (anatase) into the stable one (rutile).

Figure 6(b) also indicates that when the $TiO_2/SiO_2/GSs$ composite is calcined at the higher temperature up to 450 ℃, the larger crystal size may happen due to particle growth. The Tcal also affects not only changing the phase of TiO_2 but also bonding between TiO_2 and GSs, based on their ratio on the XRD result (Fig. 6(a)). At the Tcal at 500 ℃, the crystal size is found to be decreased, probably caused the shrinking of the structure.

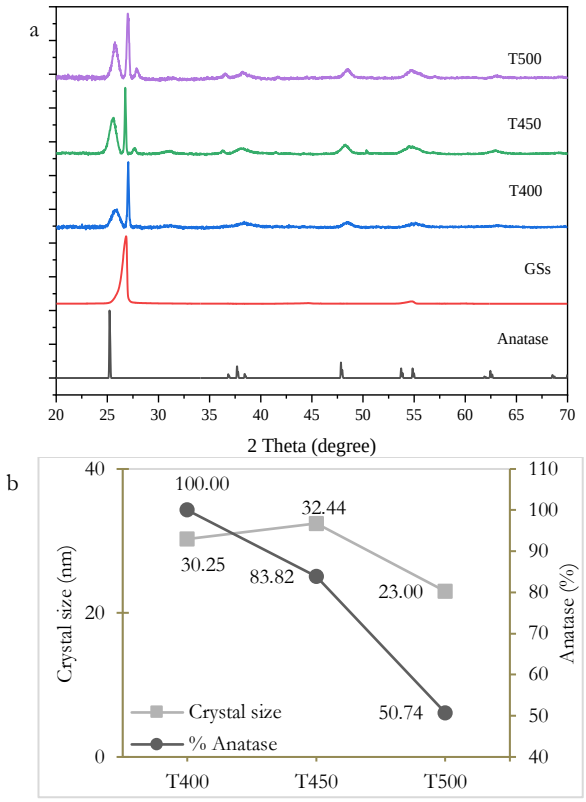

Fig. 6. (a) XRD pattern of TiO_2 photocatalyst G0.07 with a variation of Tcal and (b) the interpretation data of XRD result.

Figure 7 explains how the composition of elemental percentage, the trend for C content in the sample increases until T450 then decreases at T500. This trend shows that Tcal gives an effect on the presence of C on the sample regardless of the initial ratio of GSs; in this case, it is G0.07. It also clearly states that rutile phase on the sample affects the bonding of TiO_2 with GSs, as it shows when Tcal is 400 ℃, there is no rutile phase, and it increases at T450, proportionally with C content. However, the rutile phase is seen to increase, although the decrease of C content at T500. This behavior may involve the temperature is quite high enough to ignite the combustion reaction between carbon and oxygen in the furnace ambient. Other hand, the presence of Ti shows a random trend for each parameter. In overall results, it is suggested that the crystal size is strongly dependent on the C content, the higher

amount of C, the larger of crystal size, which clearly explains in the proposed structural model in Fig. 4.

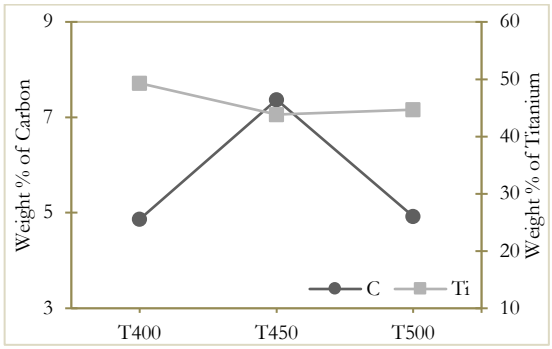

Fig. 7. EDS result of $TiO_2/SiO_2/GSs$ composite G0.07G.

The SEM image of the G0.07 TiO_2 composite is shown in Fig. 8, which can be observed how the layering of GSs was formed at different Tcal. The increase in Tcal affects the layer order. At T450, the layer started to form along with the presence of C content that is proven by EDS result. However, the layer ordering form started to less uniform with corresponding to the decreasing in C content at high temperature 500 ℃, as seen in Fig. 8 (c). Other hand, the presence of Ti shows a random trend for each parameter.

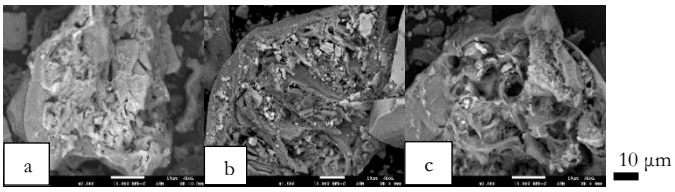

Fig. 8. SEM images of G0.07 $TiO_2/SiO_2/GSs$ composite (a) T400, (b) T450, and (c) T500.

3.2. Decolorization of Methylene Blue (MB) solution

3.2.1. Optimum condition

3.2.1.1. Effect of the light source

Light can be one of the crucial things in the photocatalytic process when the energy of light needs to be the same and or higher than the energy bandgap of the photocatalyst. In TiO_2, the energy band gap is 3.2 eV, which can be determined that ultraviolet (UV) is a suitable light. To decrease the bandgap that can be suitable to use under visible light range, this works focused on adding carbon (GSs). Figure 9 shows that G0.04T500 can do photocatalytic decolorization of MB under solar light with an efficiency of 90.3 % within 3 hours. In the dark condition, the concentration decreases remarkably because of the MB adsorption to the $TiO_2/SiO_2/GSs$ surface. It be color-changing [30]. The efficiency of adsorption under dark conditions can be reached by 84.84 % within 3 hours.

For comparison, degradation under a specified LED lamp also taken place. It shows no different results from the test under dark conditions. It means that under LED lamp, the main process that is happened is adsorption, like dark condition. Meanwhile, solar light gives quite high results since it has a broad wavelength which helpful enough for photocatalyst. Reaction under UV lamp also was done to provide a brief result on how TiO_2 photocatalyst reacts under its work range. The result shows that in the first 1 hour of reaction, more than 86 % of MB was adsorbed and degraded.

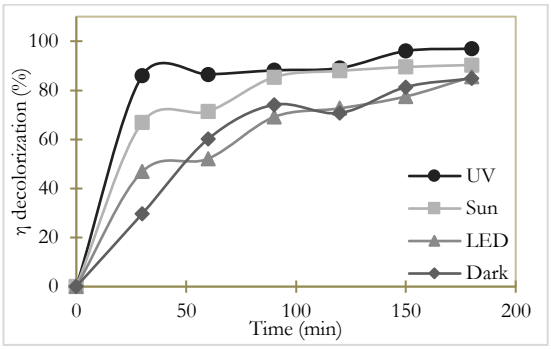

Fig. 9. The effect of decolorization under four conditions; dark, UV lamp (366 nm), solar light, and LED lamp on TiO_2 G0.04T500.

The adsorption on photocatalyst has an important role in the photocatalytic process. TiO_2 adsorb MB in their surface before photocatalytic degradation takes place. In this experiment, the observation of decolorization under dark condition can show how the adsorption of $TiO_2/SiO_2/GSs$ photocatalyst occurs. In this step, the photocatalytic degradation did not happen due to the lack of energy from light and the surface of the photocatalyst would be saturated by MB. Meanwhile, under light conditions (UV, LED, and solar), the efficiency of decolorization slightly higher than in the dark condition because there was a photocatalytic degradation process of MB into other compounds along its desorption and be replaced by other MB because of the adsorption process. Thus, for this condition at very longer time that beyond the testing time in this work, all MB molecules may be degraded by photocatalysis. However, the MB that adsorbed on the catalyst surface under dark condition may still exist as the attached surface molecules.

The process under dark condition can be remarked as an adsorption process of $TiO_2/SiO_2/GSs$ photocatalyst. Figure 10 shows how the adsorption occurred in the first 1 hour of reaction. If it is compared to the EDS result of the amount of C content at the same Tcal, it does show the same trend for T400 yet starts not to display a similar tendency with the adsorption at T450 and higher. Instead, it shows that at some point in Tcal for the same ratio, the adsorption process decreases. In overall results, the maximum adsorption capacity is for G0.07T450, which is relating to the crystal size of 34.26 nm and 83.82 %

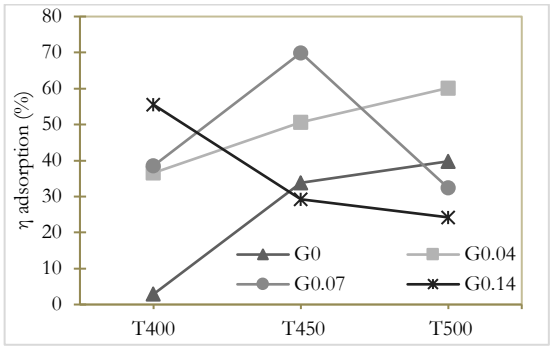

Fig. 10. Adsorption of TiO_2/SiO_2/GSs under the dark condition for each ratio and Tcal.

3.2.1.2. Effect of the amount of TiO_2/SiO_2/GSs photocatalyst

The photocatalytic degradation is determined with a variation of TiO_2/SiO_2/GSs catalyst loading in the 100 mL of MB concentration (2.5 mg/L) under solar light. The result in Fig. 11 shows that the increase in catalyst loading can increase decolorization while the exceed of catalyst (0.2 g) did not show that trend. This works can be used to determine the optimum catalyst loading for specific concentrations to avoid excess catalyst usage while getting the best efficiency result. The 0.1 g of catalyst loading G0.07T450 TiO_2/SiO_2/GSs for 100 mL of 2.5 mg/L MB generates the best decolorization of 97.83 % within 3 hours.

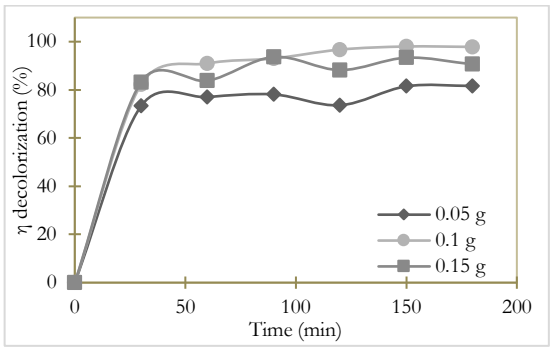

Fig. 11. The effect of the amount of TiO_2 photocatalyst for decolorization of MB.

3.2.1.3. Effect of the initial concentration of MB

With the fixed catalyst loading (0.1 g TiO_2/SiO_2/GSs /100 mL MB), the initial concentration gives an effect of decolorization efficiency. Figure 12 shows how the result of the lowest concentration (1 mg/L) has a similar outcome with 2.5 mg/L (97-99 %), while for the highest one (4 mg/L), it drops to 56 %. It shows how the excess concentration of MB leads to the overcapacity of the photocatalyst in a specific amount. This result can be concluded that as to 2.5 mg/L MB, it shows the effectiveness of 0.1 g of G0.07T450 of TiO_2/SiO_2/GSs to degrade 100 mL MB.

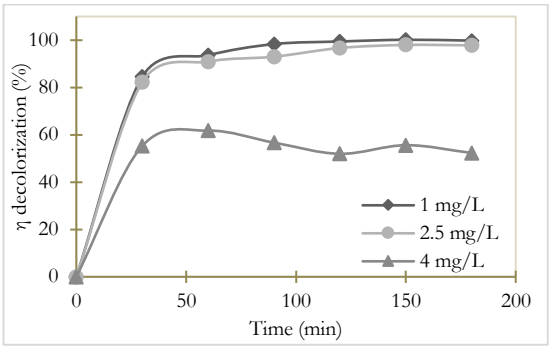

Fig. 12. The effect of concentration of MB on the decolorization process.

3.2.2. Effect of GSs ratio

Figure 17 shows how each sample gave a different result of the decolorization based on color under solar light for 1 hour. This color can provide a brief result then can be compared after a UV-Vis spectrophotometer analyzed it. The absorbance result can be converted to MB concentration and calculated η decolorization for each time range by Eq. (4). Figure 13 shows how the TiO_2/SiO_2/GSs with different ratio of GSs affects the decolorization of MB.

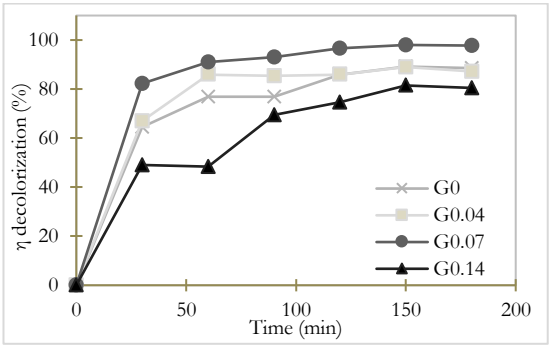

Fig. 13. The effect of ratio Ti:GSs to η decolorization (%) for T450.

The result shows that G0.07T450 gives the best result of photocatalytic activity under solar light for the degradation of MB. It also implies that the photocatalytic activity of TiO_2/SiO_2/GSs gives the best on a ratio of anatase: rutile phase 83.8 %:16.2 % and the optimum C content on the sample is 7.96 %w. The more C content does not give a better result of decolorization of MB because G0.07 and G0.14 have a similar ratio of anatase: rutile while the C content is different.

The result of degradation can determine how the kinetics of the reaction. By using Eq. (5), the rate constant of each ratio can be calculated, which is shown in Fig. 14(a). The highest rate constant for a photocatalytic reaction is G0.07T450 at 0.0201 min-1. Later, the value of the rate constant was used to calculate the model of degradation rate for each sample. Then this model data was compared to the experiment data, as shown in Fig. 14(b), where the lines represent model data, and the symbols are experiment data. It exhibits the model

DOI:10.4186/ej.2021.25.6.1

equation of LH is reasonable to describe the experimental data for all tests in this work.

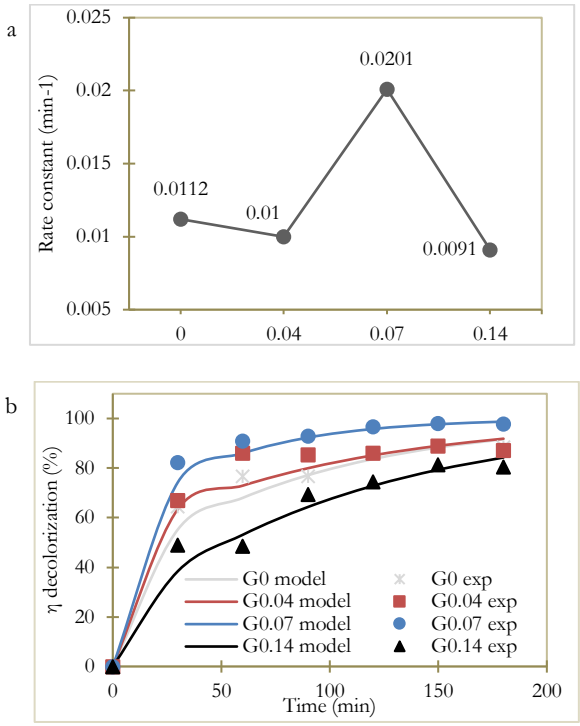

Fig. 14. (a) The rate constant of $TiO_2/SiO_2/GSs$ for each ratio at T450 and (b) validity between experiment data and model data.

As in the photocatalyst, there are considering two separate processes (adsorption and photocatalytic degradation), the rate constant is distinguished by k_1 and k_2 by the value shown in the Table 1.

Table 1. k_1 and k_2 and k of LH eq for $TiO_2/SiO_2/GSs$ for each ratio at T450.

Sample	k_1 (min^{-1})	k_2 (min^{-1})	k_1/k_2	k (LH eq) (min^{-1})
G0	0.0077	0.0094	0.819149	0.0112
G0.04	0.0088	0.0127	0.692913	0.01
G0.07	0.012	0.0122	0.983607	0.0201
G0.14	0.0032	0.0027	1.185185	0.0091

These results show that the value of k_1 is similar as k_2 for MB concentration of 2.5 mg/L. It explains that the adsorption of MB into the layer of $TiO_2/SiO_2/GSs$ composite has occurred simultaneously with the photocatalytic degradation of MB in the layer of photocatalyst at the same time. k value from LH equation is added to compare how the rate constant of photocatalytic activity will change when one process (adsorption) is neglected. It seems like k from LH eq is slightly higher than k_1 and k_2.

3.2.3. Effect of Tcal

Tcal plays a significant contribution to give a different structure of TiO_2 that can affect the photocatalytic activity. Figure 15 shows the effect of Tcal for G0.07 of $TiO_2/SiO_2/GSs$. The result shows the highest decolorization was by T450 with 97.83 % decolorization.

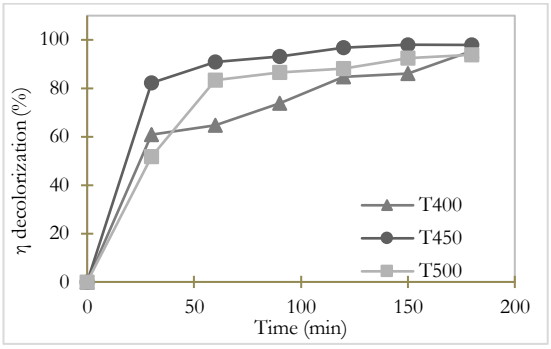

Fig. 15. The effect of Tcal on η decolorization for G0.07 $TiO_2/SiO_2/GSs$.

T450 gives the best result on the decolorization of MB under solar light. It shows how the crystal phase of TiO_2 gives an effect of degradation since T400 is pure anatase gives the lowest η decolorization compare to other Tcal, which has developed a rutile phase on TiO_2. The amount of C content, since there is a combustion reaction at high temperature, was lower at 500 °C, though it has a high rutile phase, decolorization of MB was lower than T450. Figure 16(a) gives the rate constant of G0.07 for each Tcal. Then the rate constant was used to calculate the model data for the degradation rate of each sample, to be plotted in Fig. 16(b), and compared with the experimental data.

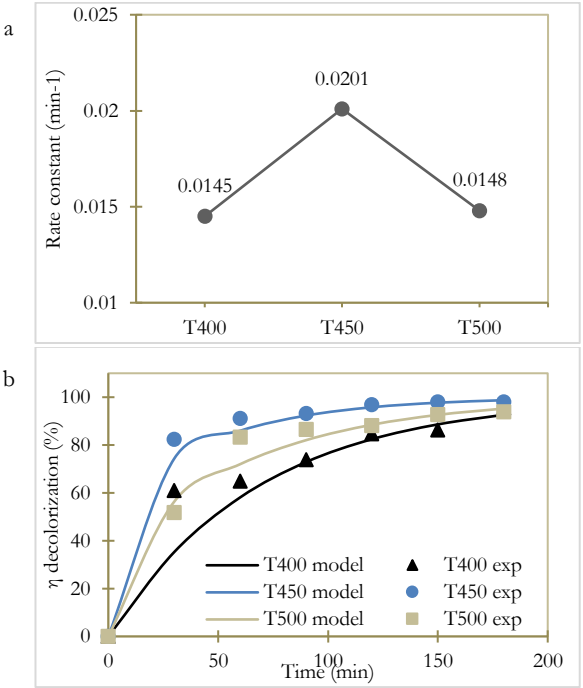

Fig. 16. (a) The rate constant of G0.07 $TiO_2/SiO_2/GSs$ for each Tcal and (b) validity between experiment data and model data.

Table 2 shows the value of k_1 and k_2 of G0.07 TiO_2/SiO_2/GSs for each Tcal. This value of k_1 is similar with k_2 for MB concentration of 2.5 mg/L. It explains that the adsorption of MB into layer of TiO_2 composite is occurred simultaneously with the photocatalytic degradation of another MB.

Table 2. k_1 and k_2 and k of LH eq for G0.07 TiO_2/SiO_2/GSs for each Tcal

Sample	k_1 (min^{-1})	k_2 (min^{-1})	k_1/k_2	k (LH eq) (min^{-1})
T400	0.0118	0.0191	0.617	0.0145
T450	0.012	0.0122	0.983	0.0201
T500	0.0039	0.0027	1.444	0.0148

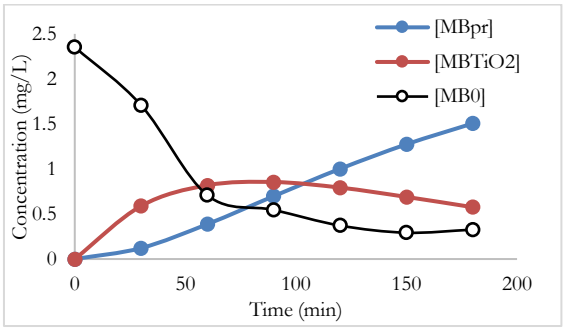

Fig. 17 Concentration changes of MB_0, MB_{TiO2}, MB_{pr} in photocatalytic degradation by G0.07T450 TiO_2/SiO_2/GSs

In Fig. 17, the value of k_1 and k_2 of G0.07T450 are applied into Eq. (13) and (14) to know the concentration [MB] at any time. It shows that the concentration of [MB_{TiO2}] rises then falls toward zero meanwhile the concentration of [MB_{pr}] rises from zero to the concentration of [MB_0]. Most of the TiO_2/SiO_2/GSs composite have rate constant k_2 quite higher than k_1. In this case, the adsorption process tends to slower than the photocatalytic degradation process.

Figure 18 shows the photographic images of blank MB and in the presence of TiO_2/SiO_2/GSs photocatalyst after 60 min of solar irradiation. MB in the presence of TiO_2/SiO_2/GSs was started to decolorize after 60 min, especially for sample G0.07T450 that was nearly colorless. The results confirm that the presence of an optimum amount of GSs in TiO_2/SiO_2/GSs enhances the degradation of MB under solar light.

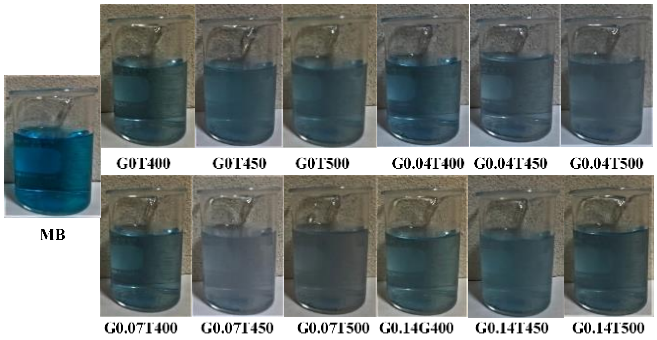

Fig. 18. Comparison of decolorization of MB for each composition and Tcal under solar light for 1 hour.

3.2.4. Effect of reusable/stability

Generally, the photocatalyst is stable and can be used several times until its particle is damaged. The experiment to test the reusable of the photocatalyst was conducted as following, after G0.07T450 TiO_2/SiO_2/GSs used for degradation of MB was completed for the first batch, the photocatalyst was washed by ethanol and following by water to neutralize the pH then heated at 100 ℃ to remove the water. This 0.1 g reused photocatalyst was used to degrade a new MB solution at a fixed initial concentration of 2.5 mg/L for 3 hours under solar light. This activity was observed for three cycles. Figure 18 shows the decolorization efficiency of the second drop from the first cycle to reach 93.1 %, then the third cycle drops to 92.4 % and drops again with the fourth one at 87.65 %. However, the efficiency slightly decreases, the differences could be due to the error during the washing of photocatalyst. From this series of experiments, it could be confirmed that the G0.07T450 photocatalyst has a stable structure and can be used several times. Therefore, it is suitable to use in many applications.

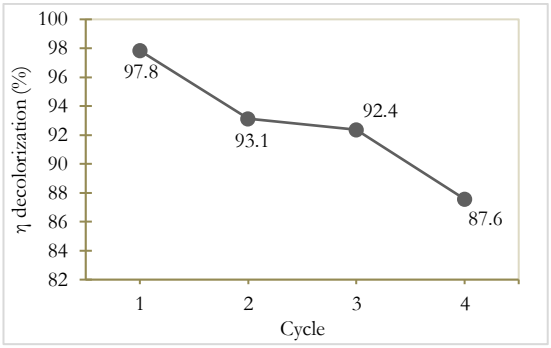

Fig. 19. Effect of recycled of G0.07T450 TiO_2 photocatalyst to η decolorization.

3.2.5. Mechanism of TiO_2/SiO_2/GSs photocatalyst

The mechanism of semiconductor photocatalyst is based on the energy of the bandgap between valence band and conductive band. TiO_2 is a semiconductor that has 3.2 eV bandgap energy, which makes this work as photocatalyst on the UV work range. The doping of GSs

DOI:10.4186/ej.2021.25.6.1

in this research was done to decrease the bandgap so it can work on the visible light spectrum. Carbon on GSs in the form of hexagonal lattice is attracted to the oxygen on TiO_2 then formed dipole-dipole force between them. This bond was explained in Fig. 19. The bond produces a dipole moment, which disturbs the stability of bonding in TiO_2 and reduces the bandgap on TiO_2 [31]. The bonding between oxygen on TiO_2 and oxygen on SiO_2 has happened. The bandgap decrease is affected by a defect that occurs in TiO_2. It is supported by how the crystal size of $TiO_2/SiO_2/GSs$ composite is bigger than TiO_2/SiO_2 (G0) which is affected by GSs presence that make a defect into TiO_2 and create the state of dipole moment into bandgap as shown in Fig. 2. That makes $TiO_2/SiO_2/GSs$ composite can work as a photocatalyst under solar light (visible light range). SEM images in Fig. 5 also give the observation of how the layer of $TiO_2/SiO_2/GSs$ is affected along with the ratio of GSs, the more GSs the more defect that appeared.

The testing of $TiO_2/SiO_2/GSs$ as photocatalyst was done by doing a degradation of methylene blue dye under solar light. The mechanism of photocatalytic degradation later was explained in Fig. 20 [1, 17, 26, 32, 33]. In the figure, it can explain how the presence of GSs affects the bandgap of TiO_2, the energy of solar light can fill the gap to excite the electron into conduction band and the photocatalytic reaction has occurred. Meanwhile, TiO_2/SiO_2 without GSs has a 3.2 eV bandgap that only can be used under a UV lamp (387 nm or less) [9, 30]. When it be used under solar light, the decreasing of pollutant concentration can occur since there was an adsorption process in TiO_2/SiO_2 photocatalyst. Also, there was a UV work range in solar light (3-5 %) that can activate the photocatalytic reaction. Furthermore, the percentage anatase-rutile phase, the ratio of GSs in composite, and morphology such as crystal size can also affect the photocatalytic activity.

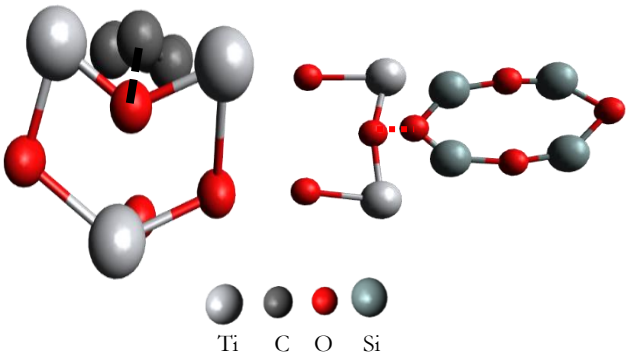

Fig. 20. Bonding on $TiO_2/SiO_2/GSs$ photocatalyst.

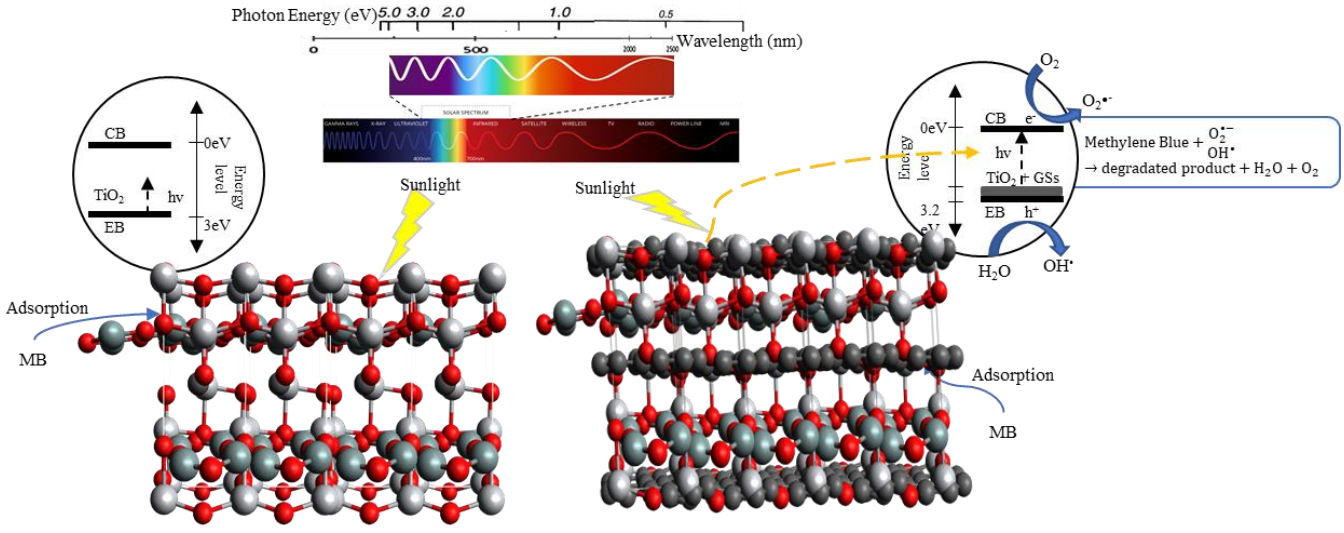

Fig. 21. Mechanism of photocatalytic degradation of MB by $TiO_2/SiO_2/GSs$ composite.

4. Conclusion

$TiO_2/SiO_2/GSs$ composite was prepared by the sol-gel method, followed by a calcination step. The morphology was investigated at different ratio Ti:GSs compositions and calcination temperature (Tcal). $TiO_2/SiO_2/GSs$ composite shows the layer pattern was affected by the presence of GSs, while the EDS spectrum confirms the existence of Ti and C on the surface of the composite. With an increase in the amount of GSs, average crystal size and percentage of rutile phase tendency increase, whereas anatase phase decreases.

Meanwhile, the increase in Tcal only affects the increasing percentage of rutile phase. The average crystal size tends to increase with the increase in Tcal until 450 ℃ and then shrink at 500 ℃. The degradation of MB shows a good result of photocatalytic activity under solar light.

Moreover, the MB degradation using the TiO_2/SiO_2/GSs photocatalyst under solar light depends on the optimum parameters such as the crystalline phase, crystal size, and C content on the sample. The maximum efficiency of MB decolorization with 97.83 % within 3 hours is obtained from the photocatalyst prepared with Ti:GSs ratio at 0.07 and Tcal at 450 ℃ (G0.07T450). The ability of reusable TiO_2/SiO_2/GSs shows a slight decrease in efficiency after four cycle times.

Acknowledgment

All these works are financially supported by a SUT-Ph. D Scholarship Program for ASEAN from Suranaree University of Technology.

References

[1] M. Castellote and N. Bengtsson, "Principles of TiO_2 Photocatalysis," in *Appl. Titan. Dioxide Photocatal. to Constr. Mater. State-of-the-Art Rep. RILEM Tech. Comm. 194-TDP*, Y. Ohama and D. Van Gemert, Eds. Springer Netherlands, Dordrecht, Springer, Apr. 2011, vol. 5, pp. 5–10.

[2] M. Umar and H. A. Aziz, "Photocatalytic degradation of organic pollutants in water," in *Org. Pollut.*, M. N. Rashed, Ed. Rijeka: IntechOpen, 2013.

[3] M. Pawar, S. Topcu Sendoğdular, and P. Gouma, "A brief overview of TiO_2 photocatalyst for organic dye remediation: Case study of reaction mechanisms involved in Ce-TiO_2 photocatalysts system," *J. Nanomater.*, vol. 2018, Jan. 2018.

[4] J. Oudenhoven, F. Scheijen, and M. Wollfs, "Fundamental of photocatalytic water splitting by visible light," in *Visible Light - Active Photocatalysis: Nanostructured Catalyst Design, Mechanisms, and Applications*. Wiley Online, 2004, ch. 3, pp. 1–22.

[5] M. A. Barakat and R. Kumar, "Photocatalytic activity enhancement of titanium dioxide nanoparticles," in *Photocatalytic Act. Enhanc. Titan. Dioxide Nanoparticles Degrad. Pollut. Wastewater*. Springer International Publishing, Cham, 2016, pp. 1–29.

[6] V. Augugliaro, G. Palmisano, L. Palmisano, and J. Soria, "Heterogeneous photocatalysis and catalysis: An overview of their distinctive features," in *Heterog. Photocatal.*, G. Marcì and L. Palmisano, Eds. Elsevier, 2019, ch. 1, pp. 1–24.

[7] S. Zhu and D. Wang, "Photocatalysis: Basic principles, diverse forms of implementations and emerging scientific opportunities," *Adv. Energy Mater.*, vol. 7, no. 23, Aug. 2017.

[8] L. Liu and Y. Li, "Understanding the reaction mechanism of photocatalytic reduction of CO_2 with H_2O on TiO_2-based photocatalysts: A review," vol. 14, no.2, pp. 453-469, Mar. 2014.

[9] A. Jain and D. Vaya, "Photocatalytic activity of TiO_2 nanomaterial," *J. Chil. Chem. Soc.*, vol. 62, no. 4, pp. 3683–3690, Feb. 2017.

[10] P. Huo, P. Kumar, and B. Liu, "The mechanism of adsorption, diffusion, and photocatalytic reaction of organic molecules on TiO_2 revealed by means of on-site scanning tunneling microscopy observations," *Catalysts*, vol. 8, no. 12, Dec. 2018.

[11] A. M. Pennington, "Increased visible-light photocatalytic activity of TiO_2 via band gap manipulation," M.S. thesis, Rutgers Univ, New Brunswick, New Jersey, 2015.

[12] X. Kang, S. Liu, Z. Dai, Y. He, X. Song, and Z. Tan, "Titanium dioxide: From engineering to applications," *Catalysts*, vol. 9, 191, 2019.

[13] J. Schneider, M. Matsuoka, M. Takeuchi, J. Zhang, Y. Horiuchi, M. Anpo, and D. W. Bahnemann, "Understanding TiO_2 photocatalysis: Mechanisms and materials," *Chem. Rev.*, vol. 114, no. 19, pp. 9919–9986, Sep. 2014.

[14] J. S. Dalton, P. A. Janes, N. G. Jones, J. A. Nicholson, K. R. Hallam, and G. C. Allen, "Photocatalytic oxidation of NOx gases using TiO_2: A surface spectroscopic approach," *Environ. Pollut.*, vol. 120, no. 2, pp. 415–422, Dec. 2002.

[15] R. Singh and S. Dutta, "Synthesis and characterization of solar photoactive TiO_2 nanoparticles with enhanced structural and optical properties," *Adv. Powder Technol.*, vol. 29, no. 2, pp. 211–219, Feb. 2018.

[16] M. Najafi, A. Kermanpur, M. R. Rahimipour, and A. Najafizadeh, "Effect of TiO_2 morphology on structure of TiO_2-graphene oxide nanocomposite synthesized via a one-step hydrothermal method," *J. Alloys Compd.*, vol. 722, pp. 272–277, Oct. 2017.

[17] B. Tang, H. Chen, H. Peng, Z. Wang, and W. Huang, "Graphene modified TiO_2 composite photocatalysts: Mechanism, progress and perspective," *Nanomaterials*, vol. 8, no. 2, Feb. 2018.

[18] S. Au–pree, P. Narakaew, S. Thungprasert, T. Promanan, A. Chaisena, and S. Narakaew, "Enhanced photocatalytic activity of C-doped TiO_2 under visible light irradiation: A comparison of corn starch, honey, and polyethylene glycol as a carbon sources," *Engineering Journal*, vol. 25, no. 1, pp. 53-68, Jan. 2021.

[19] Y. Zhang, Z. R. Tang, X. Fu, and Y. J. Xu, "TiO_2-graphene nanocomposites for gas-phase photocatalytic degradation of volatile aromatic pollutant: is TiO_2-graphene truly different from other TiO_2-carbon composite materials?," *ACS Nano.*, vol. 4, no. 12, pp. 7303–7314, Nov. 2010.

[20] L. J. Zhou, S. S. Yan, B. Z. Tian, J. L. Zhang, and M. Anpo, "Preparation of TiO_2-SiO_2 film with high photocatalytic activity on PET substrate," *Mater. Lett.*, vol. 60, no. 3, pp. 396–399, Feb. 2006.

[21] R. A. Aziz, I. Sopyan, "Synthesis of TiO_2-SiO_2 powder and thin film photocatalysts by sol-gel method," *Indian J. Chem. Sect. A—Inorganic Bio-Inorganic Phys. Theor. Anal. Chem.,* vol. 48A, pp. 951–957, Jul. 2009.

[22] K. Rachanon "Removal of air pollutants by photocatalytic process using TiO_2-SiO_2 coated dan kwian pottery," (in Thai) M.S. thesis, Chem. Eng., SUT, Nakhon Ratchasima, Thailand, 2013. [Online]. Available: http://sutir.sut.ac.th:8080/jspui/handle/123456789/4751

[23] A. Haider, Z. N. Jameel, and Y. Taha, "Synthesis and characterization of TiO_2 nanoparticles via sol- gel method by pulse laser ablation," *Eng. &Tech. Journal*, vol. 33, Part (B), no. 5, pp. 761-771, Nov. 2015.

[24] N. Boonprakob, W. Chomkitichai, J. Ketwaraporn, A. Wanaek, B. Inceesungvorn, and S. Phanichphant, "Photocatalytic degradation of phenol over highly visible-light active BiOI/TiO_2 nanocomposite photocatalyst," *Engineering Journal*, vol. 21, no. 1, pp. 81-91, Jan. 2017.

[25] Y. Rufai, S. Chandren, and N. Basar, "Influence of solvents, polarity on the physicochemical properties and photocatalytic activity of titania synthesized using deinbollia pinnata leaves," *Front. Chem.*, vol. 8, Dec. 2020.

[26] A. Eshaghi, R. Mozaffarinia, M. Pakshir, and A. Eshaghi, "Photocatalytic properties of TiO_2 sol-gel modified nanocomposite films," *Ceram. Int.*, vol. 37, no. 1, pp. 327–331, Jan. 2011.

[27] V. Kumar, K. Porkodi, and F. Rocha, "Langmuir Hinshelwood kinetics – A theoretical study," *Catal. Commun.*, vol. 9, no. 1, pp. 82–84, Jan. 2008.

[28] R. Giovannetti, E. Rommozzi, C. Anna D'Amato, and M. Zannotti, "Kinetic model for simultaneous adsorption/photodegradation process of Alizarin Red S in water solution by nano-TiO_2 under visible light," *Catalysts*, vol. 6, no. 84, pp. 1-9, Jun. 2016.

[29] H. Zhang, F. Li, Q. Jia, and G. Ye, "Preparation of titanium carbide powders by sol–gel and microwave carbothermal reduction methods at low temperature," J. Sol-Gel Sci. Technol., vol. 46, pp. 217–222, Feb. 2008.

[30] R. J. Tayade, T. S. Natarajan, and H. C. Bajaj, "Photocatalytic degradation of methylene blue dye using ultraviolet light emitting diodes," *Ind. Eng. Chem. Res.*, vol. 48, no. 23, pp. 10262–10267, Oct. 2009.

[31] C. Shang, B. Xu, X. Lei, S. Yu, D. Chen, M. Wu, B. Sun, G. Liu, and C. Ouyang, "Bandgap tuning in MoSSe bilayers: Synergistic effects of dipole moment and interlayer distance," *Phys. Chem. Chem. Phys.*, vol. 20, no. 32, pp. 20919–20926, Jul. 2018.

[32] S. G. Kumar and L. G. Devi, "Review on modified TiO_2 photocatalysis under UV/visible light: Selected results and related mechanisms on interfacial charge carrier transfer dynamics," *J. Phys. Chem. A.*, vol. 115, no. 46, pp. 13211–13241, Sep. 2011.

[33] S. Dutta, S. A. Parsons, C. Bhattacharjee, P. Jarvis, S. Datta, and S. Bandyopadhyay, "Kinetic study of adsorption and photo-decolorization of Reactive Red 198 on TiO_2 surface," *Chem. Eng. J.*, vol. 155, no. 3, pp. 674–679, Dec. 2009.

Mia Lestari Ayuningtyas was born in Manado, Sulawesi, Indonesia in 1992. She received the B.S. degree in Nuclear Chemical Engineering from Polytechnic Institute of Nuclear Technology, Indonesia, in 2014. She currently is a Ph.D. candidate in material engineering, Suranaree University of Technology, Thailand. Her previous research focussed on nanomaterial M41S for radiopharmaceuticals purpose. Her research interest now are include nanomaterials and photocatalyst.

Ms. Mia Lestari Ayuningtyas was a recepient of the SUT-Ph.D. scholarship for ASEAN at Suranaree University of Technology in 2015.

Supunnee Junpirom received the B.S. and Ph.D degrees in Chemical Engineering from Suranaree University of Technology (SUT), Nakhon Ratchasima, Thailand, in 2000 and 2007, respectively. From 2009 she has been a lecturer in School of Chemical Engineering, SUT. Her research interests include activated carbon, photocatalysis, catalytic dehydration of ethanol, low-temperature sterilization and production of polylactic acid. She has got more than 10 publications in national and international journals.

Sukasem Watcharamaisakul is an assistant professor at the school of ceramic engineering, institute of engineering, at the Suranaree University of Technology. He is also head of graduate program in biomedical innovation engineering. He received his D.Eng. from the division of materials science and engineering, the Hokkaido University in 2003. His research interest is in advanced ceramic materials, biomaterials, photocatalytics, nanomaterials and composite materials.